Editors' Suggestion

Detection of Quantum Interference without an Interference Pattern

Iliya Esin,[1] Alessandro Romito,[2] and Yuval Gefen[3]
[1]Physics Department, Technion, 3200003 Haifa, Israel
[2]Department of Physics, Lancaster University, Lancaster LA1 4YB, United Kingdom
[3]Department of Condensed Matter Physics, The Weizmann Institute of Science, Rehovot 76100, Israel

(Received 31 October 2019; accepted 21 May 2020; published 10 July 2020)

Quantum interference is typically detected through the dependence of the interference signal on certain parameters (path length, Aharonov-Bohm flux, etc.), which can be varied in a controlled manner. The destruction of interference by a which-path measurement is a paradigmatic manifestation of quantum effects. Here we report on a novel measurement protocol that realizes two objectives: (i) certifying that a measured signal is the result of interference avoiding the need to vary parameters of the underlying interferometer, and (ii) certifying that the interference signal at hand is of quantum nature. In particular, it yields a null outcome in the case of classical interference. Our protocol comprises measurements of cross-correlations between the readings of which-path weakly coupled detectors positioned at the respective interferometer's arms and the current in one of the interferometer's drains. We discuss its implementation with an experimentally available platform: an electronic Mach-Zehnder interferometer (MZI) coupled electrostatically to "detectors" (quantum point contacts).

DOI: 10.1103/PhysRevLett.125.020405

Introduction.—Quantum interferometry differs from its classical counterpart in its sensitivity to "which-path" detection. In classical wave interference, the wave amplitude can be observed along individual interfering trajectories without affecting the interference itself. Quantum mechanically, information on the trajectory traveled by the interfering particle destroys the interference pattern. This is a specific example of the adverse effect of quantum measurement: it is an invasive operation, accompanied by backaction of the detector on the system's state [1,2] and, in the case of strong (projective) measurement, it leads to the collapse of the system's wave function [3]. As far as establishing the fact that interference, classical or quantum, takes place, common wisdom is that this requires continuous variation of a control parameter [e.g., interferometer arm's length, Aharonov Bohm (AB) flux for charged particles [4]]. The observation of interference *and* of the collapse of the coherent wave function to a state that does not exhibit an interference pattern (following which-path detection) are a manifestation of the quantum nature of the phenomenon. Such combined measurements have been demonstrated in studies of average currents of electronic interferometers [5–9], and analyzed theoretically for single-electron [10,11] and many-body [12,13] protocols. The question addressed here is of a fundamental nature: can one detect particle interference avoiding the need to vary an external parameter, *and* verify that the interference signal is inherently of a quantum nature?

Here we report on a quantum measurement protocol that is used to certify the presence of quantum interference through an interferometer without varying the interferometer's parameters. We make use of minimally invasive (weak) which-path measurements and their correlations with the interferometer signal. The nonlocality of the which-path measurements provides us access to the individual wave packets that make the interference signal. Continuous (weak) measurements allow one to preserve the quantum coherence of the state since the latter is only perturbatively affected as information is being acquired by the detector [14,15]. Correlating the outcome of weak quantum measurements with a subsequent strong measurement forms the basis of weak values [16,17]; the latter has been introduced to address foundational issues [18–22] and, later on, for various applications [23–33]. A protocol involving projective which-path measurements correlated with the input signal has been shown to violate Bell-like inequalities [34]. Here we define and implement a more complex correlated measurement protocol involving simultaneous (weak) detection of which-path signals in the respective arms of the interferometer and the (strongly measured) interference signal. Our protocol provides an experimental recipe for accessing nonclassical contributions to the interference signal. At the same time, it avoids the need for measuring interference patterns and measurement induced backaction separately. Furthermore, to underscore the fact that our protocol addresses genuinely quantum effects, we demonstrate that when applied to a classical interferometer it yields a null outcome. For the sake of specificity, we outline the implementation of our protocol with an electronic MZI [35].

Setup and protocol.—Our electronic MZI has two electronic beam splitters, [a.k.a. quantum point contacts

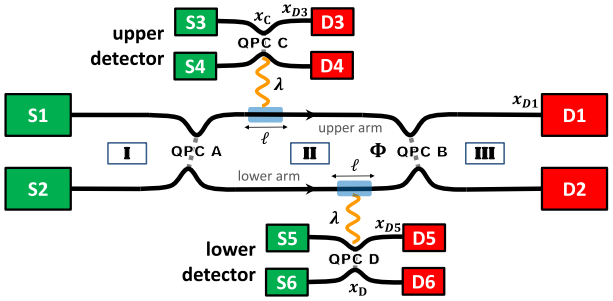

FIG. 1. A detection setup. An MZI electrostatically coupled to two QPCs C and D serving as which-path detectors. The transmission through QPC $C(D)$ is slightly modified (with a strength proportional to λ) upon the detection of a charge fluctuation in the respective MZI's arm, within a segment ℓ. The currents are measured in the drains $D1$, $D3$, and $D5$. Sector II of the MZI is threaded with a magnetic flux Φ.

(QPCs), cf. QPC A and B in Fig. 1]. The propagation of the electron through the MZI is described in terms of scattering states. For the sake of simplicity, we consider a monochromatic electron beam of energy $\hbar\omega$ that originates from the source Sn; the respective incoming state is given by

$$\psi_{mn}(x,\omega;t) = \frac{1}{\sqrt{L}} e^{-i\omega(t-x/v)} \mathcal{A}_{mn}(x,\omega), \tag{1}$$

where $\mathcal{A}_{mn}(x,\omega) = \delta_{mn}$ if $x \in I$, $\mathcal{A}_{mn}(x,\omega) = [\mathcal{S}_A(\omega)]_{mn}$ if $x \in II$, and $\mathcal{A}_{mn}(x,\omega) = [\mathcal{S}_A(\omega)\mathcal{S}_B(\omega)]_{mn}$ if $x \in III$. The sectors I, II, and III are shown in Fig. 1 and the indices $m, n = 1, 2$ label the two arms of the interferometer. For a vector state $|\psi\rangle$ denoting the amplitudes in the two arms of the MZI, the effects of QPCs A and B are described by the scattering matrices $\mathcal{S}_A = \left(\begin{smallmatrix} r_A & -t_A^* \\ t_A & r_A \end{smallmatrix}\right)$ and $\mathcal{S}_B = \left(\begin{smallmatrix} r_B & -t_B^* e^{i\chi} \\ t_B e^{-i\chi} & r_B \end{smallmatrix}\right)$, respectively. Here t_A (t_B) is the amplitude for an electron incoming from arm 1 to be transmitted to arm 2, $r_{A(B)} = \sqrt{1-|t_{A(B)}|^2}$, and $\chi = (\omega\Delta\ell/v) + 2\pi(\Phi/\Phi_0)$ is the sum of the orbital and magnetic phase differences between electrons traversing the upper and lower MZI's arms with a geometric mismatch $\Delta\ell$.

The electronic MZI is coupled, through electrostatic interactions, to two detector QPCs (cf. QPC C and D in Fig. 1). The electrons in the detectors are modeled in a similar fashion to the electrons in the MZI. It is useful to introduce the eigenmodes of QPC C:

$$\varphi_{mn}(x,\omega;t) = \frac{e^{-i\omega(t-\frac{x}{v})}}{\sqrt{L}} \begin{cases} \delta_{mn} & , x < x_C \\ [\mathcal{S}_C(\omega)]_{mn} & , x > x_C \end{cases}, \tag{2}$$

where $m, n = 3, 4$. The eigenmodes of QPC D are defined similarly, replacing C with D and setting $m, n = 5, 6$. For simplicity of notations, throughout we assume that QPCs C and D are identical. Electrostatic interactions between charges in the MZI arms and the detectors are modeled assuming that the presence of charge in the respective MZI arms slightly modifies the transmission probability of QPC C or QPC D, with strength proportional to λ. The detectors sense charge fluctuations over a segment of length ℓ in the respective interferometer arms. For simplicity, we assume equal Fermi velocities v, and lengths L of all channels, yielding the time of flight $\tau_{\rm FL} = L/v$. The sources $S1$, $S3$, and $S5$ are biased by voltage V relative to the other grounded contacts.

Inspired by the weak value protocol, which singles out quantum correlations via conditioning weak measurements [11], we define a weak-weak-strong (WWS) value of the current at the drain $D1$, conditioned on the weak detections of charges at the upper and lower arms of the MZI (see Supplemental Material [36]). The protocol relies on the readout of zero-frequency cross-correlations and expectation values of the currents at the drains $D1$, $D3$, and $D5$, which we denote by $\mathcal{I}_{D1}$, $\mathcal{I}_{D3}$, and $\mathcal{I}_{D5}$. Thereby, the WWS value is given by

$$\langle \mathcal{I}_{D1} \rangle_{\rm WWS} \equiv \langle\!\langle \mathcal{I}_{D1} \rangle\!\rangle_{D3,D5} - \langle\!\langle \mathcal{I}_{D1} \rangle\!\rangle_{D1,D1}, \tag{3}$$

where $\langle\!\langle \mathcal{I}_{D1} \rangle\!\rangle_{D3,D5} \equiv \frac{\langle \delta\mathcal{I}_{D1}\delta\mathcal{I}_{D3}\delta\mathcal{I}_{D5}\rangle}{\langle \delta\mathcal{I}_{D3}\delta\mathcal{I}_{D5}\rangle}$, and $\langle\!\langle \mathcal{I}_{D1} \rangle\!\rangle_{D1,D1} \equiv \langle (\delta\mathcal{I}_{D1})^3\rangle / \langle (\delta\mathcal{I}_{D1})^2\rangle$. Here $\delta\mathcal{I} \equiv \mathcal{I} - \langle\mathcal{I}\rangle$ denotes the fluctuations of the current around its average value $\langle\mathcal{I}\rangle$. The expectation values represent the low-frequency component of the signal and are obtained by averaging over a time window τ, which we assume to be larger than all characteristic timescales of the experiment ($\tau \gg \tau_{\rm FL}, \hbar/eV$). For example, the three-current correlator is defined as

$$\langle \delta\mathcal{I}_{D1}\delta\mathcal{I}_{D3}\delta\mathcal{I}_{D5}\rangle \equiv \lim_{\substack{\omega_1\to 0 \\ \omega_2 \to 0}} \frac{1}{\tau^2} \iint_{-\tau/2}^{\tau/2} dt_1 dt_2 e^{i\omega_1 t_1} e^{i\omega_2 t_2} \mathcal{G}_{135}(t_1,t_2), \tag{4}$$

where $\mathcal{G}_{135}(t_1,t_2) \equiv \langle \delta\mathcal{I}_{D1}(0)\delta\mathcal{I}_{D3}(t_1)\delta\mathcal{I}_{D5}(t_2)\rangle$.

Single-particle analysis.—To lay out the concept, we first analyze a simplified single-particle picture. Physically, this corresponds to a dilute current scenario, where the distance between consecutive electron wave packets is larger than their spatial width [37]. We also assume energy-independent transmission amplitudes, i.e., $\mathcal{A}_{mn}(x,\omega) \equiv \mathcal{A}_{mn}(x)$. In the absence of the detectors, the current at drain Dm, $m = 1, 2$, which originates from a voltage biased source Sn, $n = 1, 2$ is obtained via the Landauer-Büttiker formalism [38,39], $\langle \mathcal{I}_{Dm}\rangle = (e^2V/h)|\mathcal{A}_{mn}(x_{Dm})|^2$. Employing the definition of $\mathcal{A}_{mn}$ [introduced in Eq. (1)], the current can be expressed in terms of the scattering matrices $\mathcal{S}_A$, $\mathcal{S}_B$ as $\langle \mathcal{I}_{Dm}\rangle = \langle Sn|\mathcal{I}_{Dm}|Sn\rangle$, where $\mathcal{I}_{Dm} = (e^2V/h)\mathcal{S}_A^\dagger\mathcal{S}_B^\dagger\mathcal{P}_{Dm}\mathcal{S}_B\mathcal{S}_A$. Here $\mathcal{P}_{Dm} = |Dm\rangle\langle Dm|$ and $|Sn\rangle$, $|Dm\rangle$ are vector states (cf. the definition of $\mathcal{S}_A$ and $\mathcal{S}_B$) corresponding to the electron at source Sn and drain Dm, respectively (e.g., $|S1\rangle = |D1\rangle = (\,1 \quad 0\,)^T$).

We unfold our Hilbert space in the system (MZI-detectors product space). Specifically, we consider the propagation of a wave packet incident from the source $S1$, along with electrons in $S3$ and $S5$. The incident state is thus $|\Psi\rangle = |S1, S3, S5\rangle$. The interaction between the system and the upper detector is described by the scattering matrix of the QPC C, $\mathcal{S}_C = \left(\begin{smallmatrix} \check{r}^\dagger & -\check{t}^\dagger \\ \check{t} & \check{r} \end{smallmatrix}\right)_C$, where the subscript C in the definition of $\mathcal{S}_C$ indicates that the matrix is defined in the subspace of QPC C. The elements of $\mathcal{S}_C$ ($\check{r}$ and $\check{t}$) are matrices acting in the subspace of the MZI, representing the dependence of the transmission amplitude of QPC C on the position of a wave packet in the MZI. Here, $\check{t} = t_0 \cdot \mathbb{1}_{\mathrm{MZI}} + \lambda \mathcal{P}_C$, where t_0 is the transmission of an isolated detector, $\mathbb{1}_{\mathrm{MZI}}$ is the unity matrix in the MZI subspace, and $\mathcal{P}_C = \left(\begin{smallmatrix} 1 & 0 \\ 0 & 0 \end{smallmatrix}\right)_{\mathrm{MZI}}$ is the projector to the upper MZI's arm. The small parameter λ controls the strength of the weak system-detector coupling. The matrix $\check{r}$ is a diagonal matrix in the subspace of MZI satisfying $\check{r}^\dagger\check{r} + \check{t}^\dagger\check{t} = \mathbb{1}_{\mathrm{MZI}}$. Note that each element of $\mathcal{S}_C$ is a 2×2 matrix in the Hilbert subspace of the MZI's arms so that $\mathcal{S}_C$ describes both the effect of the system on the detector signal and the backaction onto the system.

Similar considerations apply for the coupling of the system and the lower detector, via charge-sensitive transmission of QPC D, replacing the index C with D, and employing $\mathcal{P}_D = \left(\begin{smallmatrix} 0 & 0 \\ 0 & 1 \end{smallmatrix}\right)_{\mathrm{MZI}}$. Analogously to the current at $D1$, the currents at $D3$ and $D5$ are defined by the expectation values of the matrices $\mathcal{I}_{D3} = (e^2V/h)\mathcal{S}_C^\dagger \mathcal{P}_{D3}\mathcal{S}_C$, and $\mathcal{I}_{D5} = (e^2V/h)\mathcal{S}_D^\dagger \mathcal{P}_{D5}\mathcal{S}_D$ on the injected state $|\Psi\rangle$, with $\mathcal{P}_{Dm}$ projectors on the arm Dm.

We are now in a position to evaluate the WWS value of Eq. (3) within the single-particle framework, $\langle \mathcal{I}_{D1}\rangle^{\mathrm{SP}}_{\mathrm{WWS}}$. To compute this quantity we need the three-current correlator of Eq. (3), which requires the ordering of the scattering matrices and the projectors along the wavelets' paths; these act from the sources $S1, S3, S5$ towards the drains $D1, D3, D5$ and backwards,

$$\langle \mathcal{I}_{D1}\mathcal{I}_{D3}\mathcal{I}_{D5}\rangle = \left(\frac{e^2V}{h}\right)^3 \langle \Psi|\mathcal{S}_A^\dagger \mathcal{S}_C^\dagger \mathcal{S}_D^\dagger \mathcal{S}_B^\dagger \mathcal{P}_{D1}\mathcal{P}_{D3}\mathcal{P}_{D5}\mathcal{S}_B\mathcal{S}_D\mathcal{S}_C\mathcal{S}_A|\Psi\rangle. \tag{5}$$

Likewise, in order to obtain an explicit form of $\langle \mathcal{I}_{D1}\rangle^{\mathrm{SP}}_{\mathrm{WWS}}$ we need to compute the correlators $\langle \mathcal{I}_{D3}\mathcal{I}_{D5}\rangle$, $\langle (\mathcal{I}_{D1})^3\rangle$, $\langle (\mathcal{I}_{D1})^2\rangle$ and expectation values of currents in terms of the scattering matrices $\mathcal{S}_B$, $\mathcal{S}_D$, $\mathcal{S}_C$, $\mathcal{S}_A$ expanded to the leading order in λ, and substitute in Eq. (3). The expression can be simplified considerably assuming t_0 and λ to be real [36], leading to the lowest order in λ to

$$\langle \mathcal{I}_{D1}\rangle^{\mathrm{SP}}_{\mathrm{WWS}} = -\frac{\langle [[\mathcal{I}_{D1}, Q_C], Q_D]\rangle}{4\langle Q_C\rangle\langle Q_D\rangle}. \tag{6}$$

Here $Q_{C(D)} = (e^2V/h)(\ell/v)\mathcal{S}_A^\dagger \mathcal{P}_{C(D)}\mathcal{S}_A$ is an operator measuring the charge sensed by the upper (lower) detector. Note that the expression in Eq. (6) is constant in λ by construction, as the numerator and the denominator in the definition of $\langle\!\langle \mathcal{I}_{D1}\rangle\!\rangle_{D3,D5}$ [see below Eq. (3)] are of the same leading order in λ. We employ the explicit expressions of the charge and current operators to rewrite Eq. (6) as

$$\langle \mathcal{I}_{D1}\rangle^{\mathrm{SP}}_{\mathrm{WWS}} = -\frac{e^2V}{h}\frac{\mathfrak{Re}\{e^{i\chi}t_A t_B^* r_A r_B\}}{2|t_A r_A|^2}. \tag{7}$$

Many-particle analysis.—The above single-particle analysis can be generalized to include a scenario where many particles are present and detected in the interferometer's arms. Throughout the following, we still discard electron-electron interaction within the MZI and within the detectors, yet account for the detection process (comprising interaction between a detector's electron and a MZI electron). The most important facet we want to include by accounting for such many-particle physics is that signals detected by the detectors and at the MZI drains may refer to different electrons (as opposed to partial waves of the same injected electron). Our formalism needs to rid of such spurious contributions. Departing from a single-particle framework, we replace the Landauer-Büttiker approach by full-fledged time-dependent operator averages in Eq. (3), evaluated within the Keldysh formalism. The three-current correlator (computed in the interaction picture, with the MZI and the detectors being uncoupled) reads

$$\langle \hat{\mathcal{I}}_{D1}(0)\hat{\mathcal{I}}_{D3}(t_1)\hat{\mathcal{I}}_{D5}(t_2)\rangle = \langle \mathcal{T}_K e^{-(i/\hbar)\oint \hat{\mathcal{H}}_{\mathrm{MD}}(t')dt'}\hat{I}_{D1}(0)\hat{I}_{D3}(t_1)\hat{I}_{D5}(t_2)\rangle. \tag{8}$$

Here $\mathcal{T}_K$ is the time-ordering operation (along the Keldysh time contour) acting on the Keldysh-symmetrized current operators in the interaction picture, $\hat{I}_{Dm}(t) = \hat{U}_0^\dagger(t)\hat{\mathcal{I}}_{Dm}(0)\hat{U}_0(t)$, $m = 1, 3, 5$, where $\hat{U}_0(t)$ is the evolution operator with respect to the Hamiltonian of uncoupled MZI and detectors.

Quantum and thermal averaging is performed with respect to the density matrix $\hat{\varrho}(-\infty)$, describing the state of the impinging electrons [emitted from the (possibly finite temperature) voltage biased reservoir], and the decoupled detectors C and D: $\hat{\varrho}(-\infty) = \hat{\varrho}_{\mathrm{MZI}}(-\infty) \otimes \hat{\varrho}_{\mathrm{QPC\,C}}(-\infty) \otimes \hat{\varrho}_{\mathrm{QPC\,D}}(-\infty)$. The density matrix of the isolated MZI is expressed as

$$\hat{\varrho}_{\mathrm{MZI}}(-\infty) = \prod_{n,\omega}[f_n(\omega)\hat{c}_n^\dagger(\omega)\hat{c}_n(\omega) + \bar{f}_n(\omega)\hat{c}_n(\omega)\hat{c}_n^\dagger(\omega)], \tag{9}$$

where $\hat{c}_n^\dagger(\omega)$, $n = 1, 2$ is an operator creating an electron in the state $\psi_{mn}(x,\omega;t)$ [Eq. (1)], $f_n(\omega) = (1 + e^{(\hbar\omega-\mu_n)/k_BT})^{-1}$ is the Fermi distribution of the electrons injected at Sn, where T and μ_n are, respectively, the temperature and the chemical potential of the lead Sn, and $\bar{f}_n(\omega) \equiv 1 - f_n(\omega)$. The density matrices of the detectors have analogous expressions with $c_n^\dagger(\omega)$, $n = 3, 4, 5, 6$ defined through Eq. (2).

The current operator near $D1$ at time t reads $\hat{I}_{D1}(t) = v\hat{\rho}_1(x_{D1};t)$, where the density operator $\hat{\rho}_m(x;t) = \hat{\psi}_m^\dagger(x;t)\hat{\psi}_m(x;t)$ and $\hat{\psi}_m^\dagger(x;t) = (\tau_{\rm FL}/2\pi)\int d\omega\psi_{mn} \times (x,\omega;t)\hat{c}_n^\dagger(\omega)$ is an operator creating an electron in the mth arm, at the position x and time t. Throughout, we implicitly sum over repeated indices. In order to express Eq. (4) in the frequency domain, and given the time averaging in Eq. (4), all operators therein should be evaluated at the same frequency, ω. Coherent superpositions of different frequency components can then be ignored, which allows us to use $\hat{\rho}_m(x;t) = (\tau_{\rm FL}/2\pi)\times \int d\omega[\rho_m(x,\omega;t)]_{nl}\hat{c}_n^\dagger(\omega)\hat{c}_l(\omega)$, where $[\rho_m(x,\omega;t)]_{nl} = e\psi_{mn}(x,\omega;t)\psi_{ml}^*(x,\omega;t)$. In turn, we are able to express the current operator as

$$\hat{I}_{D1}(t) = \frac{h}{\mathrm{eV}}\int\frac{d\omega}{2\pi}[\mathcal{I}_{D1}(\omega)]_{mn}\hat{c}_m^\dagger(\omega)\hat{c}_n(\omega). \quad (10)$$

Analogous expressions hold for the detectors' currents $\hat{I}_{D3}(t)$, $\hat{I}_{D5}(t)$. The matrices $\mathcal{I}_{Dm}(\omega)$ are frequency-dependent generalizations of the matrices $\mathcal{I}_{Dm}$ appearing in the single-particle expressions, e.g., Eq. (5).

The coupling between the MZI and the detectors is expressed through the Hamiltonian

$$\hat{\mathcal{H}}_{\rm MD}(t) = \frac{\hbar}{e^2}(\tilde{\lambda}\hat{\Gamma}_C(t)\hat{Q}_C(t) + \tilde{\lambda}\hat{\Gamma}_D(t)\hat{Q}_D(t)). \quad (11)$$

Here the charge and tunneling current operators are $\hat{Q}_C(t) = \int_{x\in\ell} dx\hat{\rho}_1(x;t)$, and $\hat{\Gamma}_C(t) = (\tau_{\rm FL}/2\pi)\int d\omega \times [\tilde{\Gamma}_C(\omega;t)]_{mn}\hat{c}_m^\dagger(\omega)\hat{c}_n(\omega)$, respectively, where $[\tilde{\Gamma}_C(\omega;t)]_{mn} = iev\varphi_{3m}(x_C^-,\omega;t)\varphi_{4n}^*(x_C^+,\omega;t) + \mathrm{H.c.}$ Analogous expressions hold for $\hat{Q}_D(t)$ and $\hat{\Gamma}_D(t)$, upon changing $C \leftrightarrow D$ and the respective channel indices.

We evaluate the correlator in Eq. (8) to leading order in $\tilde{\lambda}$ employing Eqs. (9)–(11). Similarly, we compute the other correlators in Eq. (3). To obtain the WWS value in the many-body picture, $\langle\mathcal{I}_{D1}\rangle_{\rm WWS}^{\rm MB}$, we average the correlators over time according to Eq. (4) [36]. The results are presented in Fig. 2 as a function of the interference control phase, χ.

In the low-temperature regime, $eV \gg k_BT$, we find $\langle\mathcal{I}_{D1}\rangle_{\rm WWS}^{\rm MB}|_{eV\gg k_BT} = \frac{h}{\tau|eV|}\langle\mathcal{I}_{D1}\rangle_{\rm WWS}^{\rm SP}$. The right-hand side represents the single-particle result weighted with the statistical probability of having a correlated noise, given

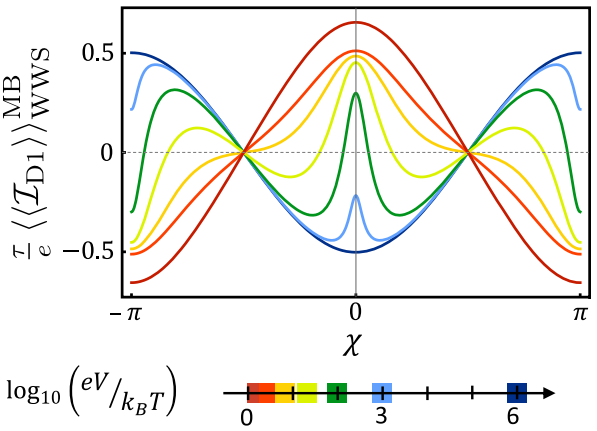

FIG. 2. The WWS value, $\langle\mathcal{I}_{D1}\rangle_{\rm WWS}^{\rm MB}$ as function of the phase difference between the two arms, χ, with transmission amplitudes $t_A = \sqrt{0.55}$ and $t_B = \sqrt{0.5}$, for several values of eV/k_BT. The WWS value oscillates around zero when varying χ. In the two limiting cases, $eV/k_BT \gg 1$ and $eV/k_BT \ll 1$, the WWS value is proportional to $\langle\mathcal{I}_{D1}\rangle_{\rm WWS}^{\rm SP}$ [Eq. (7)], albeit with different proportionality coefficients. The latter reflect the temperature dependence of the two- and three-point correlation functions [see Eq. (S20) in the Supplemental Material [36]].

that $\tau e|V|/h$ independent particles are injected during the measurement time, τ. In the opposite, high-temperature limit, the signal converges to $\langle\mathcal{I}_{D1}\rangle_{\rm WWS}^{\rm MB}|_{eV\ll k_BT} = -(2hk_BT/|eV|^2)\langle\mathcal{I}_{D1}\rangle_{\rm WWS}^{\rm SP}$, with a prefactor reflecting the thermal noise and a reversed overall sign. The sign reversal arises from the change of the relative strengths of the two terms contributing to the WWS signal in Eq. (3), following the analysis of the decoupled two- and three-point correlation functions [36]. In both of these limits, $\langle\mathcal{I}_{D1}\rangle_{\rm WWS}^{\rm MB}$ oscillates around zero when varying χ, but the oscillatory pattern changes nontrivially in the crossover from low to high temperature due to many-body (thermal noise) effects.

Quantum vs classical interference.—As demonstrated in Fig. 2, the three-point correlation function studied here assumes nonvanishing values for generic parameters of the interference setup. In fact, a nonzero value of $\langle\mathcal{I}_{D1}\rangle_{\rm WWS}$ is a direct signature of the quantum nature of the interference process. In order to confirm this we show that our three-point correlator [Eq. (3)] vanishes identically for two distinct classical scenarios: interference of classical waves, and (probabilistic, noninterfering) passage of classical particles through the interferometer arms. In both cases classical beam splitters replace the roles of the QPCs.

Consider first the case of classical particles. A particle emitted from $S1$ is scattered with probability $|t_A|^2$ onto arm 2 and remains on the same arm with probability $|r_A|^2 = 1 - |t_A|^2$. The noisy detectors have the probability $|t_0|^2$ to click in the absence and probability $|t_0|^2 + \lambda_c$ to click in the presence of a particle in the upper (lower) arm. To simplify the algebra, we set the rate of electrons injected

at the detectors equal to the rate W of electrons impinging at the beam splitter A. We further assume that W is small enough to have at most one particle in the segment between the beam splitters A and B at any instance of time.

The current correlations in this model can be determined following the same formalism outlined above (for the single-particle case), but replacing the coherent state $|\psi\rangle$ with a diagonal density matrix describing the probabilities of the classical particle to be in the respective interferometer arms. For the three-point correlator we obtain $\langle \delta\mathcal{I}_{D1}\delta\mathcal{I}_{D3}\delta\mathcal{I}_{D5}\rangle = -\lambda_c^2\mathcal{I}_0^3|t_A|^2|r_A|^2(1-2\mathcal{I})$, where $\mathcal{I} \equiv |t_A|^2|t_B|^2 + |r_A|^2|r_B|^2$ and $\mathcal{I}_0 \equiv eW$. The remaining two-point and self-correlators read $\langle \delta\mathcal{I}_{D3}\delta\mathcal{I}_{D5}\rangle = -\lambda_c^2\mathcal{I}_0^2|t_A|^2|r_A|^2$, $\langle(\delta\mathcal{I}_{D1})^3\rangle = \mathcal{I}_0^3\mathcal{I}(1-\mathcal{I})(1-2\mathcal{I})$, and $\langle(\delta\mathcal{I}_{D1})^2\rangle = \mathcal{I}_0^2\mathcal{I}(1-\mathcal{I})$. Finally, we obtain $\langle\!\langle \mathcal{I}_{D1}\rangle\!\rangle_{D1,D1} = \langle\!\langle \mathcal{I}_{D1}\rangle\!\rangle_{D3,D5}$, which, by Eq. (3), yields zero signal.

To establish a benchmark for classical waves, we consider a charge wave packet injected at $S1$ which, following the splitting at QPC A, propagates in the two arms $j = 1, 2$. The amplitude of the charge in arm 1, $Q_C(t)$, is sensed by the corresponding detector, QPC C (cf. Fig. 1) via the detector's signal $\mathcal{I}_{D3}(t) \propto |t_0|^2 + \lambda_c(\ell/v)\times Q_C(t-\tau_C)/e + \xi_3(t)$, where τ_C is the time of flight from $S1$ to the point where the charge is detected and $\xi_3(t)$ is a stochastic noise at the detector. A similar expression holds for the detector's signal $\mathcal{I}_{D5}(t)$ sensing the charge Q_D in arm 2 of the interferometer with an added noise $\xi_5(t)$. Importantly, there is no backaction here, hence the amplitudes $Q_C(t)$ and $Q_D(t)$ are unaffected by the measurement outcome (by the detectors' noise). As a result, if we assume that the wave injected at $S1$ has a stochastic component $\xi_1(t)$, the noise of the signal in $D1$ is unaffected by $\xi_3(t)$ and $\xi_5(t)$. Employing the fact that $\langle \xi_i(t)\xi_j(t')\rangle \propto \delta_{i,j}$, it follows that $\langle \mathcal{I}_{D1}\rangle_{\mathrm{WWS}} = 0$, reflecting the classical nature (no backaction) of this interferometry.

Conclusions.—We have constructed a protocol capable of addressing the "quantumness" of interference. The detection signal is nonzero in the case of quantum interference and vanishes for classical waves and for classical particles. Measurement of such a nonzero outcome above the noise level is an indication of an underlying quantum interference in the system. We have addressed both the limit of (at most) a single particle present at the interferometer at any given moment, as well as the limit of many particles present. Our protocol does not require to register a signal as a function of an externally varied parameter (e.g., the phase difference between the two arms).

Experimentally, to obtain the quantity represented by Eq. (3), four different measurements are required: the three-current cross-correlation of the currents in $D1$, $D3$, and $D5$ [cf. Eq. (5)], the two-current cross-correlation of the two detectors, and the two- and three- self-correlation functions of the current in two electronic beam splitters (QPC C and D). Note that for the electronic case both the interferometer and the QPCs operate in the quantum Hall regime, cf. Fig. 1. Given recent experimental advances in the field, we believe that our protocol can be implemented and verified in experiment. Furthermore, an intriguing follow up, both theory-wise and experiment-wise, would be the generalization of the above protocol to anyonic interferometry.

A. R. acknowledges support by EPSRC via Grant No. EP/P010180/1. Y. G. acknowledges funding from DFG RO 2247/11-1, CRC 183 (project C01), and the Minerva foundation.

[1] H. M. Wiseman and G. J. Milburn, *Quantum Measurement and Control* (Cambridge University Press, Cambridge, England, 2009).
[2] K. Jacobs, *Quantum Measurement Theory and Its Applications* (Cambridge University Press, Cambridge, England, 2014).
[3] J. V. Neumann, *Mathematical Foundations of Quantum Mechanics*, Investigations in Physics (Princeton University Press, Princeton, 1955).
[4] In principle one can assert the quantum nature of interference if the latter depends on an AB flux, which is a quantum effect *per se*. However, in practically all instances of solid-state implementations of AB interferometry, direct magnetic field, as opposed to AB flux, is applied.
[5] A. Yacoby, M. Heiblum, V. Umansky, H. Shtrikman, and D. Mahalu, Phys. Rev. Lett. **73**, 3149 (1994).
[6] E. Buks, R. Schuster, M. Heiblum, D. Mahalu, and V. Umansky, Nature (London) **391**, 871 (1998).
[7] I. Neder, M. Heiblum, D. Mahalu, and V. Umansky, Phys. Rev. Lett. **98**, 036803 (2007).
[8] J. Dressel, Y. Choi, and A. N. Jordan, Phys. Rev. B **85**, 045320 (2012).
[9] E. Weisz, H. K. Choi, I. Sivan, M. Heiblum, Y. Gefen, D. Mahalu, and V. Umansky, Science **344**, 1363 (2014).
[10] A. C. Elitzur and L. Vaidman, Found. Phys. **23**, 987 (1993).
[11] V. Shpitalnik, Y. Gefen, and A. Romito, Phys. Rev. Lett. **101**, 226802 (2008).
[12] I. Esin, A. Romito, Y. M. Blanter, and Y. Gefen, New J. Phys. **18**, 013016 (2016).
[13] O. Zilberberg, A. Romito, and Y. Gefen, Phys. Rev. B **93**, 115411 (2016).
[14] A. N. Jordan and M. Büttiker, Phys. Rev. Lett. **95**, 220401 (2005).
[15] A. A. Clerk, M. H. Devoret, S. M. Girvin, F. Marquardt, and R. J. Schoelkopf, Rev. Mod. Phys. **82**, 1155 (2010).
[16] Y. Aharonov, D. Z. Albert, and L. Vaidman, Phys. Rev. Lett. **60**, 1351 (1988).
[17] J. Dressel, M. Malik, F. M. Miatto, A. N. Jordan, and R. W. Boyd, Rev. Mod. Phys. **86**, 307 (2014).
[18] I. M. Duck, P. M. Stevenson, and E. C. G. Sudarshan, Phys. Rev. D **40**, 2112 (1989).
[19] Y. Aharonov and L. Vaidman, Phys. Rev. A **41**, 11 (1990).
[20] Y. Aharonov and L. Vaidman, J. Phys. A **24**, 2315 (1991).
[21] J. Tollaksen, Y. Aharonov, A. Casher, T. Kaufherr, and S. Nussinov, New J. Phys. **12**, 013023 (2010).

[22] Y. Aharonov, E. Cohen, and A. C. Elitzur, Phys. Rev. A **89**, 052105 (2014).
[23] N. W. M. Ritchie, J. G. Story, and R. G. Hulet, Phys. Rev. Lett. **66**, 1107 (1991).
[24] G. J. Pryde, J. L. O'Brien, A. G. White, T. C. Ralph, and H. M. Wiseman, Phys. Rev. Lett. **94**, 220405 (2005).
[25] A. Romito, Y. Gefen, and Y. M. Blanter, Phys. Rev. Lett. **100**, 056801 (2008).
[26] P. B. Dixon, D. J. Starling, A. N. Jordan, and J. C. Howell, Phys. Rev. Lett. **102**, 173601 (2009).
[27] J. S. Lundeen, B. Sutherland, A. Patel, C. Stewart, and C. Bamber, Nature (London) **474**, 188 (2011).
[28] S. Kocsis, B. Braverman, S. Ravets, M. J. Stevens, R. P. Mirin, L. K. Shalm, and A. M. Steinberg, Science **332**, 1170 (2011).
[29] E. T. F. Rogers, J. Lindberg, T. Roy, S. Savo, J. E. Chad, M. R. Dennis, and N. I. Zheludev, Nat. Mater. **11**, 432 (2012).
[30] A. Bednorz, K. Franke, and W. Belzig, New J. Phys. **15**, 023043 (2013).
[31] A. Romito and Y. Gefen, Phys. Rev. B **90**, 085417 (2014).
[32] A. N. Jordan, J. Martínez-Rincón, and J. C. Howell, Phys. Rev. X **4**, 011031 (2014).
[33] I. Esin, A. Romito, and Y. Gefen, Quantum Stud. Math. Found. **3**, 265 (2016).
[34] F. D. Santo and B. Dakić, Phys. Rev. Lett. **124**, 190501 (2020).
[35] Y. Ji, Y. Chung, D. Sprinzak, M. Heiblum, D. Mahalu, and H. Shtrikman, Nature (London) **422**, 415 (2003).
[36] See Supplemental Material at http://link.aps.org/supplemental/10.1103/PhysRevLett.125.020405 for an in-depth analysis of the relation between the WWS protocol and the weak value protocol, a detailed derivation of the WWS value, and an analysis of the correlation functions contributing to the WWS value.
[37] Here we neglect electron-electron interactions. This assumption is supported by the fact that experiments employing quantum Hall edges give rise to shot noise with Fano factor equals to 1, compatible with noninteracting electrons.
[38] R. Landauer, IBM J. Res. Dev. **1**, 223 (1957).
[39] M. Büttiker, Phys. Rev. Lett. **65**, 2901 (1990).